

## Searches for new physics produced in association to a top quark and missing transverse energy in final state.

B. ARGIENTO, ON THE BEHALF OF THE CMS COLLABORATION

*INFN, Sezione di Napoli - Napoli, Italy*

*Università degli Studi di Napoli Federico II - Napoli, Italy*

**Summary.** — Several Beyond Standard Model (BSM) theories predict final states containing top quarks produced in association with invisible particles, such as dark matter candidates, or through decays of heavy resonances like Vector-Like Quarks (VLQs). A common experimental signature among many BSM scenarios is the presence of third-generation quarks produced alongside invisible particles. This paper presents two distinct analyses: one focusing on a VLQ decaying into a top quark, and the other on dark matter production in association with single and double top quarks.

### 1. – Introduction

The Standard Model (SM) has demonstrated remarkable success in describing fundamental interactions and experimental data. However, it does not address key open questions, such as the hierarchy problem—the unexplained gap between the electroweak and Planck scales—or the quantum nature of gravity. Additionally, it lacks viable candidates for dark matter and dark energy, despite overwhelming astrophysical and cosmological evidence [1].

These limitations strongly motivate the exploration of Beyond Standard Model (BSM) physics, including theories predicting new heavy fermions such as Vector-Like Quarks (VLQs) [4] and dark matter scenarios [3] described by Simplified Models. Many of these frameworks predict final states involving third-generation quarks produced in association with invisible particles, leading to distinctive experimental signatures.

At collider experiments, quarks and gluons manifest as collimated sprays of hadrons, known as jets. The internal structure of jets—shaped by the type and kinematics of the initiating particle—plays a crucial role in identifying highly boosted heavy objects, such as top quarks or  $W/Z$  bosons, via jet substructure techniques. These methods are essential for enhancing sensitivity in searches involving energetic and partially merged decay products, as typically expected in BSM scenarios.

## 2. – CMS framework and jet reconstruction

The CMS detector[5] at LHC adopts a right-handed coordinate system with the  $z$ -axis along the beam direction,  $x$  pointing radially inward, and  $y$  upward.

The pseudorapidity  $\eta = -\log[\tan(\theta/2)]$  is used instead of the polar angle  $\theta$ , as it is invariant under boosts along the beam axis. The angular separation between particles is defined as  $\Delta R = \sqrt{(\Delta\eta)^2 + (\Delta\phi)^2}$ . Transverse momentum  $p_T = \sqrt{p_x^2 + p_y^2}$  is the most relevant observable in a hadron collider. Significant  $p_T^{\text{miss}} = -\sum_i \vec{p}_T^i$  in an event suggests momentum imbalance in the transverse plane and may indicate the production of invisible particles[6]. The analysis of such events is a key strategy in the search for new physics scenarios.

Jets are collimated sprays of hadrons originating from high-energy quarks and gluons. Their reconstruction relies on clustering algorithms; CMS mostly employs the anti- $k_T$  [7] algorithm with two typical values for the radius parameter  $R$ : **AK4 jets** ( $R = 0.4$ ), narrow jets used in resolved topologies; **AK8 jets** ( $R = 0.8$ ), large-radius jets suited for boosted objects.

In searches involving hadronically decaying top quarks, jet reconstruction adapts to the decay kinematics: **Merged**, a single AK8 jet encompassing all decay products; **Partially merged**, a  $W$ -tagged AK8 jet and a separate  $b$ -tagged AK4 jet; **Resolved**, three distinct AK4 jets. These three reconstruction strategies are illustrated in Fig. 1 and are used into the two analysis showed below.

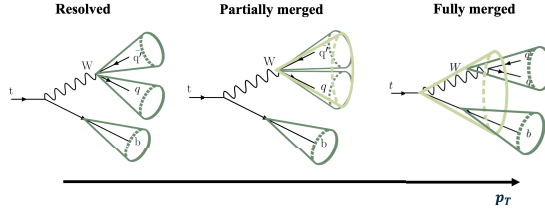


Fig. 1.: Three different reconstruction of the top quark final state in the hadronic decay.

## 3. – Vector Like Quarks - $T \rightarrow tZ(\nu\nu)$

This search targets the single production of a vector-like  $T$  quark (charge  $+2/3$ ) decaying into a top quark and a  $Z$  boson, using  $138 \text{ fb}^{-1}$  at  $\sqrt{s} = 13 \text{ TeV}$  CMS data [8]. The investigated final state is characterized by a hadronic top decay ( $t \rightarrow Wb \rightarrow q'qb$ ), a  $Z \rightarrow \nu\bar{\nu}$  decay, resulting in large  $p_T^{\text{miss}}$  and a forward jet originating from a quark emitted at low angles relative to the beam axis (Fig.2).

The analysis investigates  $T$  quark masses in the range 0.6–1.8 TeV, considering multiple hypotheses for the  $T$  quark width ( $\Gamma$ ), from 1% to 30% of its mass.

Electron and muon candidates are reconstructed in order to veto events containing isolated leptons. Offline event selection requires at least one AK4 jet with  $p_T > 30 \text{ GeV}$  and  $|\eta| < 4.0$ , as well as missing transverse momentum  $p_T^{\text{miss}} > 200 \text{ GeV}$ . To suppress multijet backgrounds, the azimuthal separation  $\Delta\phi$  between each AK4 jet and  $\vec{p}_T^{\text{miss}}$  must exceed 0.6. Events containing identified electrons or muons are rejected.

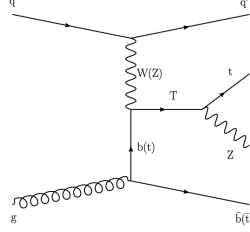


Fig. 2.: An example of a leading-order Feynman diagram showing the production of a single vector-like quark  $T$ , which decays into a  $Z$  boson and a top quark.

Top quark candidates are reconstructed using three configurations described before.

Each selected event is assigned to one of six exclusive categories, defined by the top quark reconstruction strategy (merged, partially merged, or resolved) and the presence or absence of at least one forward jet. Signal extraction is performed through a simultaneous fit to the transverse mass of the system composed of the reconstructed top quark candidate and the missing transverse momentum vector,  $M_T$ , within the six analysis categories (Fig. 3).

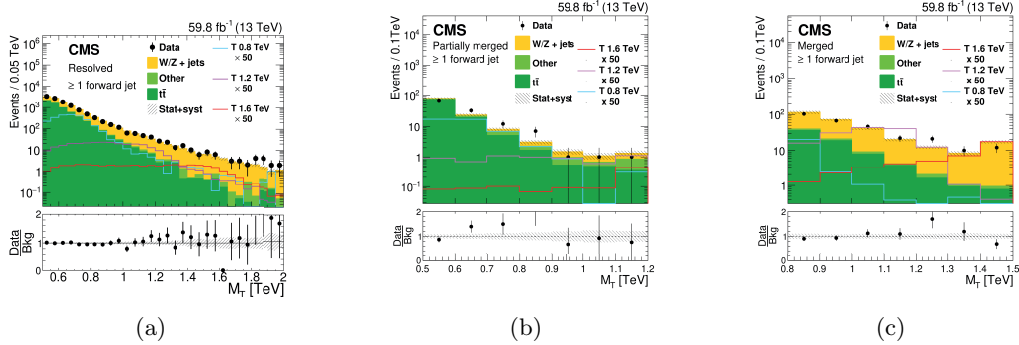


Fig. 3.: Distributions of the transverse mass  $M_T$  of the reconstructed top quark and  $\mathbf{p}_T^{miss}$  system, for the selected events in the three categories considered, for events with a forward jet for the 2018 data taking. The dominant background contributions after event selection arise from  $t\bar{t}$ +jets,  $W$ +jets, and  $Z$ +jets processes, where the  $Z$  boson decays to neutrinos

No statistically significant excess is observed in data. The most notable deviation, with a local significance of  $2.5\sigma$ , occurs for the narrow-width hypothesis at a  $T$  quark mass of  $1.4 \text{ TeV}$ . The observed and expected upper limits on the signal cross section, derived from all six event categories and shown as a function of the  $T$  quark mass  $m_T$  for various width hypotheses, are presented in Fig. 4.

#### 4. – Dark Matter - $t/\bar{t} + \text{DM}$

Simplified models offer an effective framework to describe the interactions between the SM and dark matter (DM) sectors, capturing the key kinematic features of more

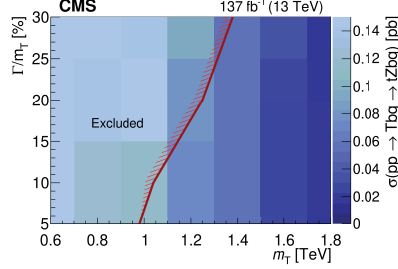


Fig. 4.: Observed 95% CL upper limits on the production cross section times branching fraction, as a function of the  $T$  quark mass. For the narrow-width hypothesis, values above 602–15  $fb$  are excluded in the 0.6–1.8  $TeV$  range. For widths between 10–30% of the mass, the excluded values range from 836 to 16  $fb$ .

elaborate theories. A common scenario involves introducing a new neutral scalar ( $\phi$ ) or pseudoscalar ( $a$ ) mediator that couples both to SM fermions and to a new Dirac fermion DM candidate ( $\chi$ ). In Fig. 5 there are the main processes involving the  $t\bar{t} + DM$  and  $t/\bar{t} + DM$  production [9] in the context of simplified model.

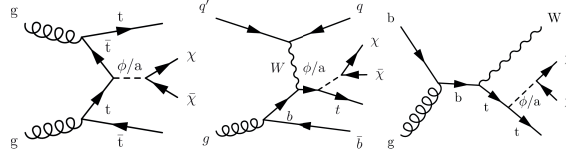


Fig. 5.: Representative leading order diagrams for the three leading production modes in the simplified model with scalar/pseudoscalar ( $\phi/a$ ) mediators: DM pair production in association with a top quark pair (left), single top via  $t$ -channel (center), and  $tW$ -channel (right).

The analysis showed in this paragraph investigates DM production in association with top quarks using the full Run 2 dataset (138  $fb^{-1}$ ) collected by the CMS experiment at  $\sqrt{s} = 13$  TeV. All the production mechanisms depicted in Fig. 5 are taken into account. Events are categorized into six signal regions based on lepton multiplicity and the presence of at least one forward jet: **All-hadronic (0 $\ell$ )**: no isolated leptons; **Single-lepton (1 $\ell$ )**: one isolated electron or muon; **Dilepton (2 $\ell$ )**: two opposite-sign leptons. As in the previous analysis, the all-hadronic region is further divided into three subregions based on top quark reconstruction (resolved, partially merged, and fully merged). Event selection emphasizes large missing transverse momentum ( $p_T^{\text{miss}} > 250$  GeV in 0 $\ell$  and 1 $\ell$  regions) and transverse mass ( $m_T > 140$  GeV in 1 $\ell$ ). In the 2 $\ell$  region, a neural network is employed to enhance discrimination, using variables such as  $\Delta\phi(\ell, \ell)$ ,  $\Delta\phi(p_T^{\text{miss}}, \ell\ell b)$ , and reconstructed  $m_{t\bar{t}}$ .

A binned maximum likelihood fit is performed across all signal and control regions using  $p_T^{\text{miss}}$  and neural network output distributions, shown in Fig. 6. Backgrounds (including  $t\bar{t}$ ,  $W$ +jets,  $Z$ +jets, and  $t\bar{t}Z$ ) are constrained using dedicated control regions.

Upper limits at 95% confidence level are derived using a modified frequentist approach with a profile likelihood test statistic in the asymptotic approximation, follow-

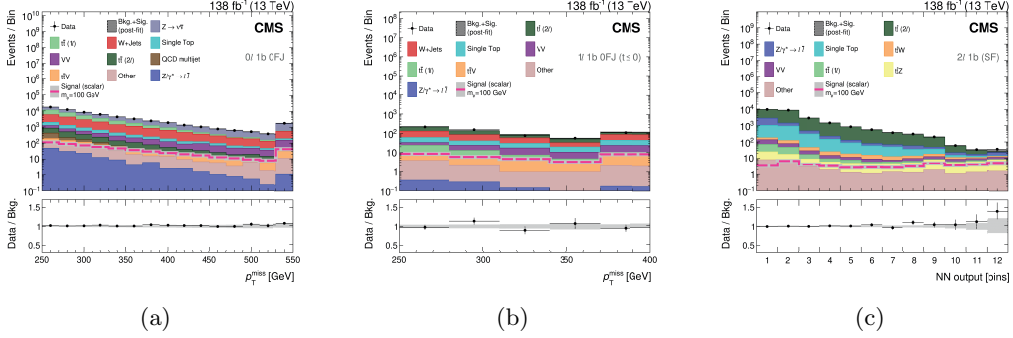


Fig. 6.: Distributions of the  $\mathbf{p}_T^{\text{miss}}$  are shown for the  $0\ell$  and  $1\ell$  categories (Fig. 6a–6b). Additionally, the main discriminant distribution of the NN is presented for the  $2\ell$  channel with same-flavor (SF, Fig. 6c) leptons in the final state. Only the categories without a forward jet are shown here are.

ing the  $\text{CL}_s$  criterion. The results are summarized in Fig. 7, which shows the model-independent upper limits on the production cross section for new physics, for both the scalar (left) and pseudoscalar (right) mediator scenarios. No significant deviation is

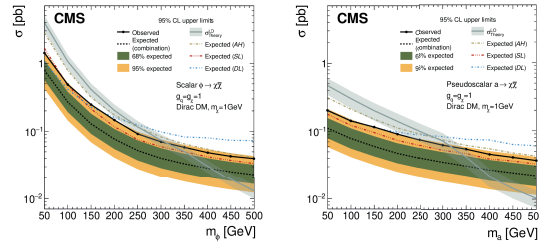


Fig. 7.: Model-independent 95% CL limits on production cross section for scalar (left) and pseudoscalar (right) interactions. Expected limits (black dashed line, with 68/95% CL green/yellow bands) and observed limits (solid black line) are shown, along with theoretical LO cross sections for the DM model (grey line).

observed. The strongest local excess corresponds to  $1.9\sigma$  for a pseudoscalar mediator of mass  $\sim 150$  GeV. At 95% CL, observed limits exclude scalar (pseudoscalar) mediator masses below  $\sim 310$  GeV (320 GeV), while expected limits reach up to 410 GeV (380 GeV). Model-independent cross section limits range from 1 pb to 0.02 pb.

## 5. – Conclusions

In conclusion, the two presented analyses probe complementary final states involving top quarks and missing transverse energy, targeting different classes of BSM scenarios. Both searches set stringent upper limits on the corresponding signal cross sections, placing robust constraints on the parameter spaces of the considered theoretical models.

In addition, recent developments within the CMS Collaboration include a novel ma-

chine learning-based algorithm named **TROTA** (*Top Reconstruction: an Object Tagger Algorithm*), designed to enhance top quark identification by combining standard reconstruction strategies (AK4 and AK8 jets) across the full kinematic regime. TROTA focuses particularly on improving the efficiency of the partially merged (mixed) category, which has traditionally presented challenges due to its intermediate topology. Preliminary results indicate that TROTA significantly improves top quark reconstruction performance (as shown in Fig. 8), demonstrating how advanced tagging strategies can further enhance the sensitivity of the analyses discussed in this work.

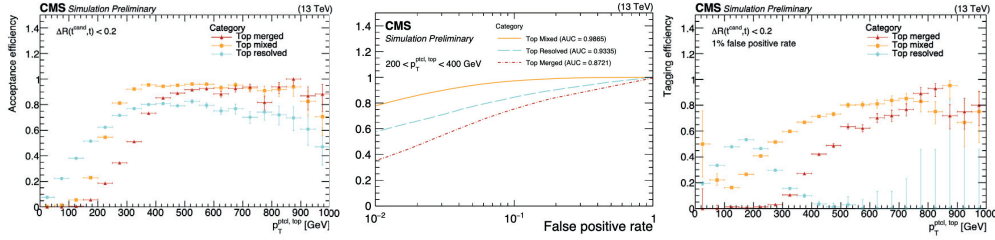


Fig. 8.: Performance of the TROTA algorithm in different reconstruction regimes. Left: Top quark reconstruction efficiency, defined as the ratio between correctly identified top quarks and the total number of true top quarks. Center: Identification performance across the resolved, mixed, and merged categories, showing improved discrimination in the resolved and mixed regions compared to the use of ParticleNet alone. Right: Overall tagging efficiency versus  $p_T$  for a fixed mistag rate of 1%; TROTA demonstrates enhanced reconstruction performance for resolved and mixed topologies, even at low  $p_T$ .

## 6. REFERENCES

- [1] G. BERTONE, D. HOOPER, and J. SILK, "Particle dark matter: evidence, candidates and constraints", *Phys. Rept.*, **405** (2005) 279, doi: 10.1016/j.physrep.2004.08.031;
- [2] M. R. BUCKLEY, D. FELD, and D. GONCALVES, "Scalar simplified models for dark matter", *Phys. Rev. D*, **91** (2015), doi:10.1103/physrevd.91.015017;
- [3] D. PINNA, A. ZUCCHETTA, M. R. BUCKLEY, and F. CANELLI, "Single top quarks and dark matter", *Phys. Rev. D*, **96** (2017) 035031, doi:10.1103/PhysRevD.96.035031;
- [4] J. A. AGUILAR-SAAVEDRA, R. BENBRIK, S. HEINEMEYER, and M. PEREZ-VICTORIA, "Handbook of vectorlike quarks: mixing and single production", *Phys. Rev. D*, **88** (2013) 094010, doi:10.1103/PhysRevD.88.094010;
- [5] CMS Collaboration, "The CMS experiment at the CERN LHC", *JINST*, **3** (2008) S08004, doi:10.1088/1748-0221/3/08/S08004;
- [6] CMS Collaboration, "Performance of missing transverse momentum reconstruction in proton-proton collisions at  $\sqrt{s} = 13$  TeV using the CMS detector", *JINST*, **14** (2019) P07004, doi:10.1088/1748-0221/14/07/P07004;
- [7] M. CACCIARI, G. P. SALAM, and G. SOYEZ, "The anti- $k_T$  jet clustering algorithm", *JHEP*, **04** (2008) 063, doi:10.1088/1126-6708/2008/04/063, arXiv:0802.1189;
- [8] CMS Collaboration, "Search for single production of a vector-like  $T$  quark decaying to a top quark and a  $Z$  boson in the final state with jets and missing transverse momentum at  $\sqrt{s} = 13$  TeV", arXiv:2201.02227 [hep-ex], 2022, arXiv:2201.02227;
- [9] CMS Collaboration, "Search for dark matter produced in association with one or two top quarks in proton-proton collisions at  $\sqrt{s} = 13$  TeV", arXiv:2505.05300 [hep-ex], 2025, arXiv:2505.05300.